Supporting Information for:
Self-Assembled ssDNA Nano-networks in Solution and at Surfaces

Miriam Simon, Albert Prause, Stefan Zauscher, Michael Gradzielski

1. Gel electrophoresis

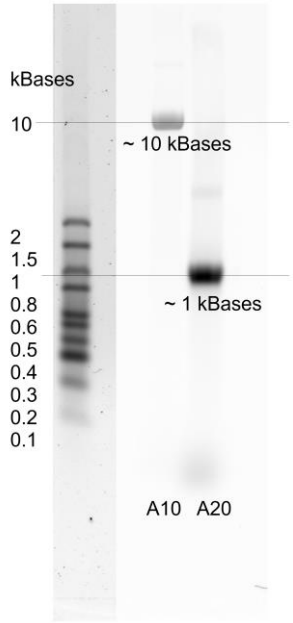

Figure S1. Exemplary gel image of two different poly(dA) strands synthesized for this work. For more examples of DNA synthesized by TdT-catalyzed enzymatic polymerization (TcEP), and information about controllability of chain length and monodispersity of this method, see Tang *et al.*[6]

2. Overlap concentration

The overlap concentration c^* is the concentration above which a molecule can no longer freely rotate in solution. Here, the overlap concentration was calculated for the two extreme conformational states: i) assuming the ssDNA to behave as a stretched chain of 1000 bases with 0.34 nm per base, yielding a contour length R_{max} of 340 nm, or ii) assuming the ssDNA to behave as a Gaussian coil, using the radius of gyration,

$$R_g = \sqrt{\frac{2 \cdot l_p \cdot R_{max}}{6}}, \tag{S1}$$

where l_p is the persistence length of 1.98 nm for ssDNA[34] and R_{max} is the contour length of 340 nm. This yields an R_g of 15 nm. The overlap concentration c^* in solution can now be calculated by:

$$c^* = \frac{1}{N_A \cdot d^3}, \tag{S2}$$

where d is the size of the molecule (here either R_{max} = 340 nm for a stretched chain or $2R_g$ = 30 nm for a Gaussian coil). The corresponding overlap concentrations in solution are, $c^*_{\mathrm{contour}} = 42$ nM and $c^*_{\mathrm{Gaussian}} = 62$ µM, respectively. Both values are well above the concentration of 9 nM used in most of our experiments. Modifying the formula for the 2D surface of a mica chip, we calculated an overlap concentration of $c^*_{\mathrm{contour}} = 0.2$ nM, suggesting that continuous network formation is possible under these conditions.

The hydrodynamic radius, R_h, of a stiff cylinder of length L and diameter D is given by the equation first developed by Broersma:[35,36]

$$R_h = \frac{L/2}{\delta - 0.5 \cdot (\gamma_{\parallel} + \gamma_{\perp})}, \tag{S3}$$

with:

$$\delta = \ln(2 \cdot \frac{L}{D}), \tag{S4}$$

$$\gamma_{\parallel} = 1.27 - 7.4 \cdot \left(\frac{1}{\delta} - 0.34\right)^2, \text{ and} \tag{S5}$$

$$\gamma_{\perp} = 0.19 - 4.2 \cdot \left(\frac{1}{\delta} - 0.39\right)^2. \tag{S6}$$

When assuming a diameter of 1 nm (ssDNA) and taking the experimental value for R_h of 15.5 nm for a single stranded polynucleotide chain, then Broersma's equation yields a length of 156 nm (or for R_h of 14.9 nm or 16.2 nm, the lengths would be 151.8 or 165 nm, respectively).

3. Additional AFM images

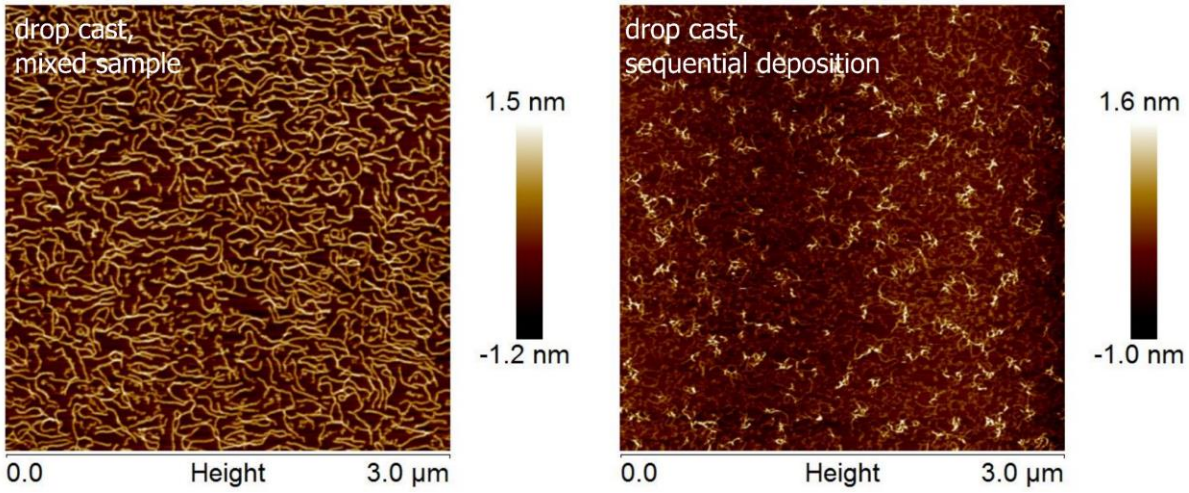

Figure S2. Self-assembled DNA network, consisting of a 50:50 mixture of poly(dA) (1 kB) and poly(dT) (1.3 kB) with a total concentration of 9 nM, prepared by the drop cast method. **A)** poly(dA) and poly(dT) were mixed in solution prior to deposition. A percolating network is visible. **B)** ssDNA deposited sequentially. In this case no percolating network is formed.

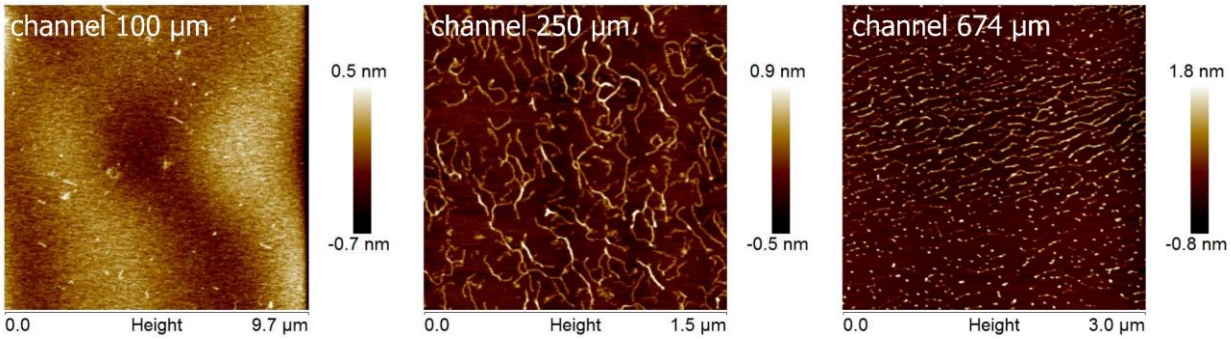

Figure S3. Deposition of DNA networks (1:1 mol ratio of poly(dA) (1 kB) and poly(dT) (1.3 kB), total c = 9 nM) using microchannels, resulted in ripped and non-continuous networks.

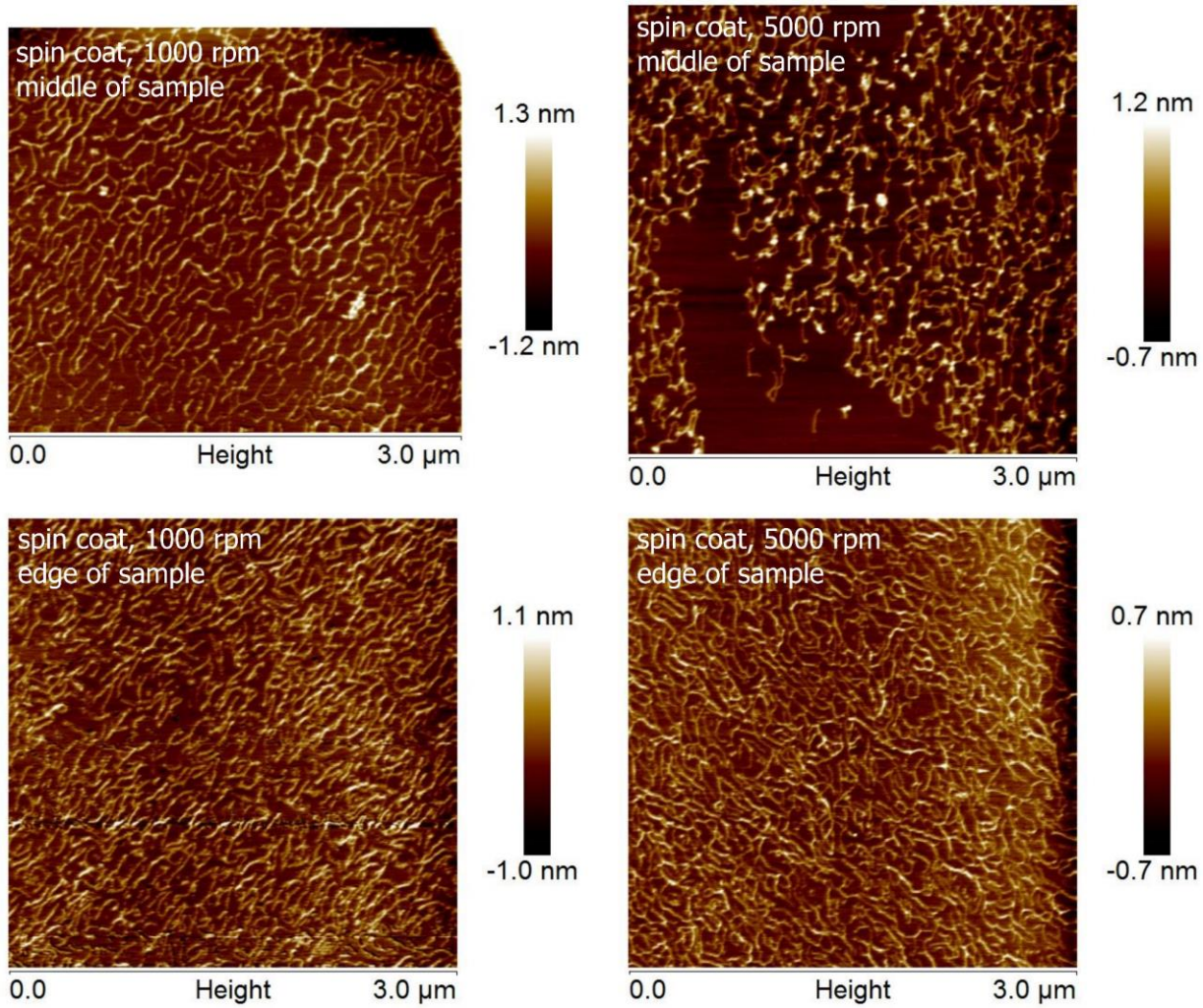

Figure S4. Deposition of DNA networks (1:1 mol ratio of poly(dA) (1 kB) and poly(dT) (1.3 kB), total c = 9 nM) using spin coating. The appearance of the network depends on its location on the mica chip. Material is being pushed to the outside and large-scale continuous networks are formed only on the periphery of the mica substrate.

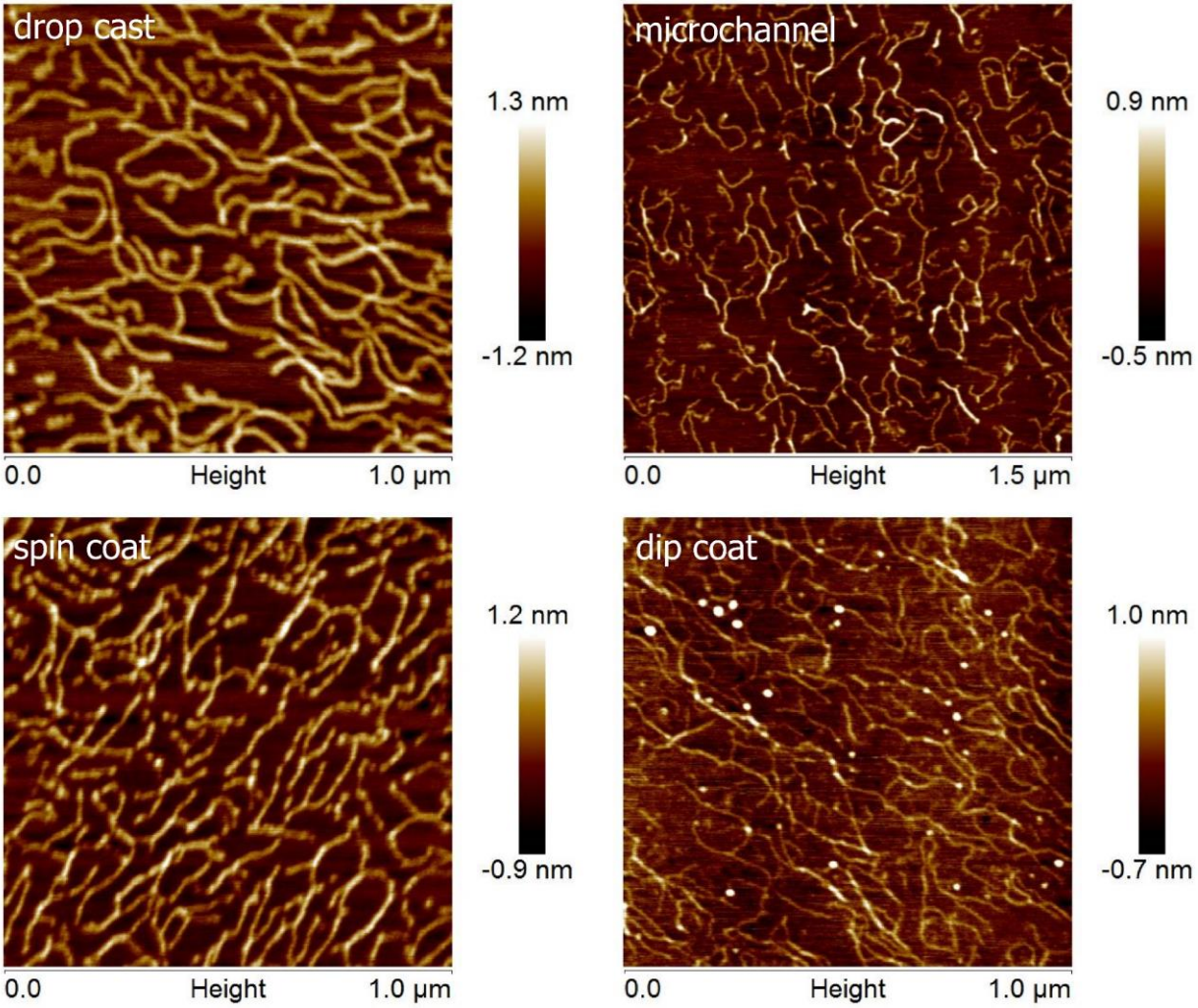

Figure S5. Comparison of different deposition methods of self-assembled DNA networks (1:1 mol ratio of poly(dA) (1 kB) and poly(dT) (1.3 kB), total c = 9 nM). Dip coating resulted in a continuous network but the DNA strands were curled and contaminated with salt crystals. The most reliable and reproducible method for large scale DNA network formation is the drop cast method described in the paper. (Compare also lower magnification image in Figure S2)

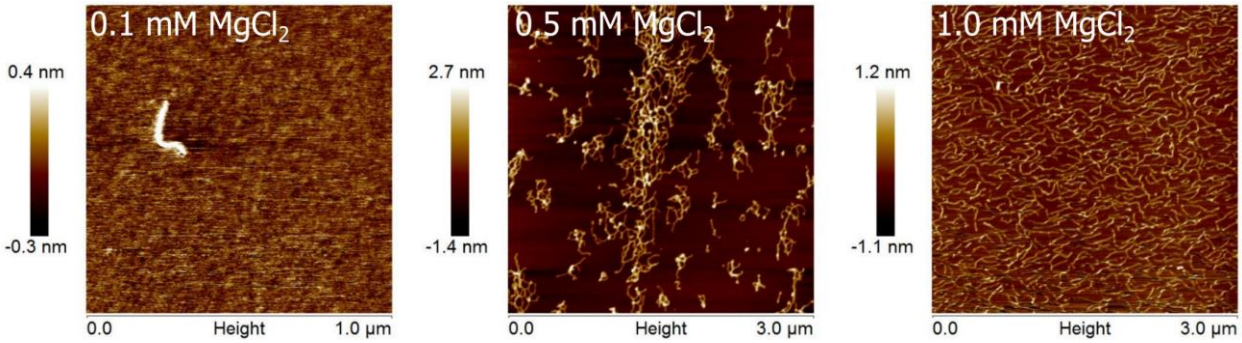

Figure S6. Enlarged AFM images from Figure 5, showing the effect of different amounts of added salt.

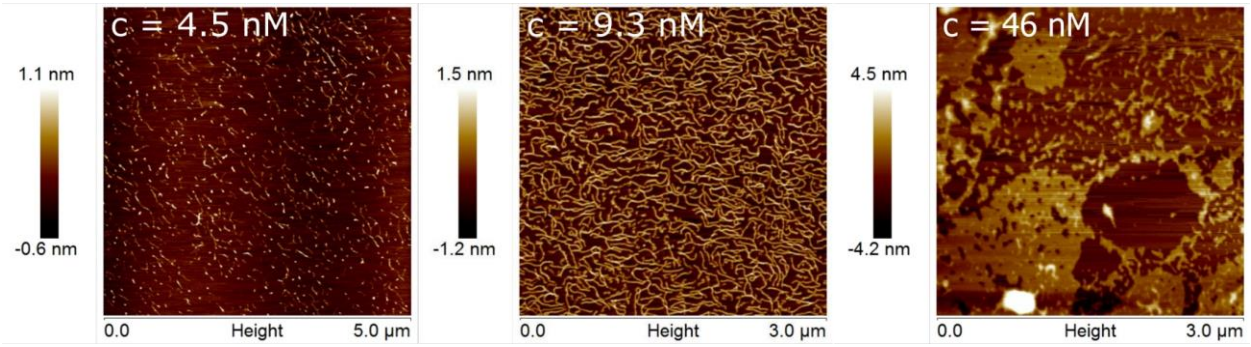

Figure S7. Enlarged AFM images from Figure 6, showing the effect of different total concentrations

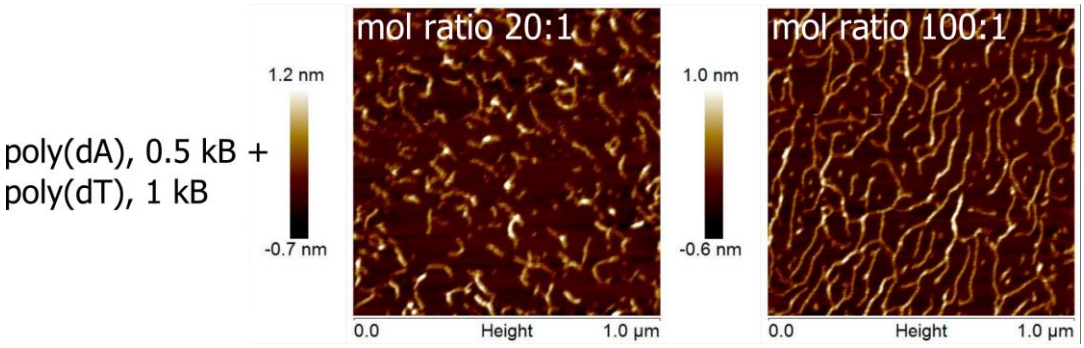

Figure S8. Enlarged AFM images from Figure 7, showing the effect of different DNA strand lengths and mixing ratios.

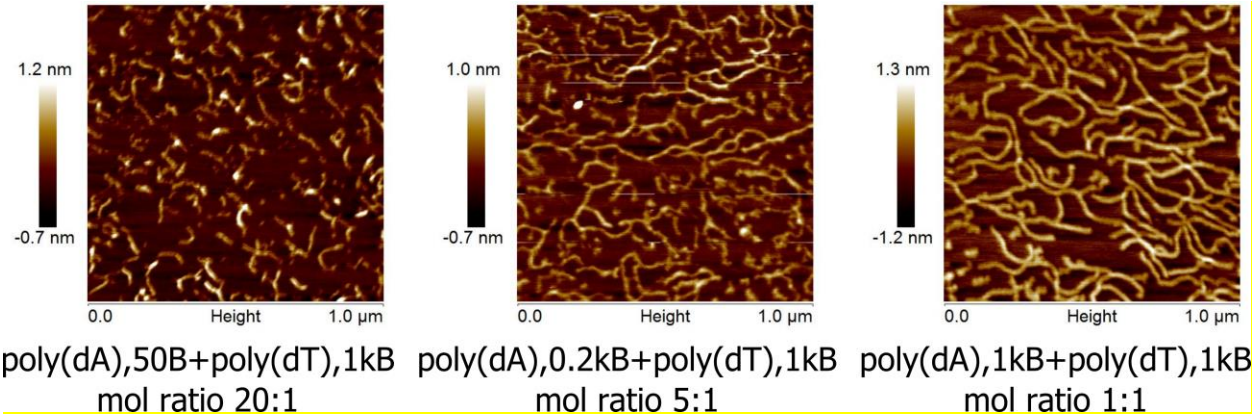

Figure S9. AFM images showing the effect of different DNA strand lengths.

4. Additional FCS/FCCS Measurements

The bimodal fitting of the FCS data was conducted similar to the monomodal formalism described in the main text. No distribution function was used here, in order not to add too many parameters to the fitting model. The bimodal correlation function is defined as:

$$G(\tau) = \sum_{i=1}^{2} \rho_i G_{D,i}(\tau, \tau_{D,i}), \tag{S7}$$

where $\langle N \rangle = \left(\sum_{i=1}^{2} \rho_i\right)^{-1}$ is the average number of fluorescent molecules in the confocal volume, $x_i = \langle N \rangle \rho_i$ the fraction of species i, and $G_{D,i}(\tau, \tau_{D,i})$ the normalized correlation function (cf. eq. 3) with τ as correlation time, $\tau_{D,i}$ the relaxation time of the species i, and k the anisotropy of the confocal volume,

$$G_{D,i}(\tau, \tau_{D,i}) = \left(1 + \frac{\tau}{\tau_{D,i}}\right)^{-1} \cdot \left(1 + \frac{\tau}{\tau_{D,i} \cdot k^2}\right)^{-\frac{1}{2}}. \tag{S8}$$

The fitting of the data was performed with a Python script.

Table S1. Fit results of all data shown in this paper: N = number of fluorophores in V_{eff}, = $1/A$, x_1 and x_2 = fraction of diffusive mode 1 and 2, $D_{f,1}$ and $D_{f,2}$ = diffusion coefficients, $R_{h,1}$ and $R_{h,2}$ = hydrodynamic radii. Standard deviations ($\pm\sigma_D$) are given in parentheses.

	N	x_1	$D_{f,1}$ / µm²/s	$R_{h,1}$ / nm	x_2	$D_{f,2}$ / µm²/s	$R_{h,2}$ / nm
poly(dAdT) cross-corr.	14.890	1	2.87(0.6)	85.4(17)			
poly(dAdT) ch1 auto	3.80	0.54	1.69(0.3)	144.9(29)	0.46	25.66(5)	9.55(2)
ss-poly(dT) ch1 auto	2.44	0.82	16.4(3.6)	14.9(3.3)	0.18	2.19(0.6)	111.9(30)
ss-poly(dA) ch2 auto	7.89	1	15.1(3.1)	16.2(3.3)			
poly(dAdT) 0.5nM	13.93	1	3.49(0.8)	70.1(15)			
poly(dAdT) 5nM	5.67	1	4.23(0.9)	57.9(12)			
poly(dAdT) 10nM	5.17	1	3.71(0.8)	66.0(13)			
poly(dAdT) 80nM	13.38	1	3.75(0.8)	65.3(13)			
poly(dAdT) 890nM	133.27	1	5.44(1.1)	45.1(9.1)			
dAdT 10nM; 1mM $MgCl_2$	3.56	1	4.69(1.0)	52.2(11)			
dAdT 10nM; 10mM $MgCl_2$	3.68	1	4.41(0.9)	55.5(11)			
dA(0.5)+dT(1.3); 2:1	9.92	1	6.37(1.3)	38.4(7.7)			
dA(0.5)+dT(1.3); 5:1	17.21	1	5.89(1.2)	41.6(8.4)			
dA(8.0)+dT(1.3); 1:6	17.79	1	13.9(2.8)	17.6(3.6)			
dA(8.0)+dT(1.3); 1:10	24.97	1	17.9(3.8)	13.7(2.9)			

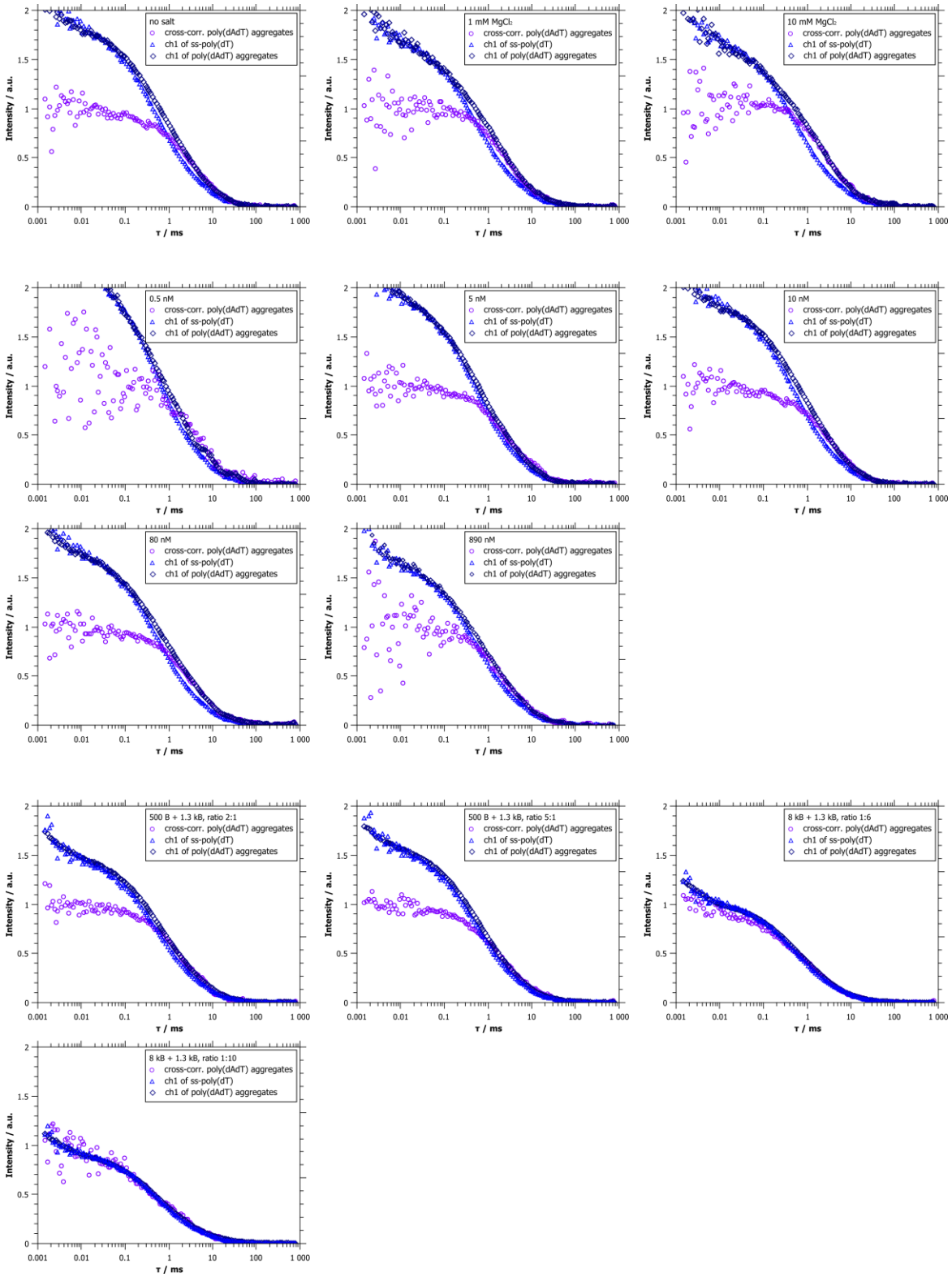

Figure S10. Auto-correlation functions of poly(dT) in poly(dAdT) aggregates (ch1 of poly(dAdT) aggregates) and the free ss-poly(dT) chains (ch1 of ss-poly(dT)) compared to the cross-correlation functions of the mixed samples (cross-corr. poly(dAdT) aggregates). It shows that the mixed samples always contain large aggregates as well as free ssDNA.

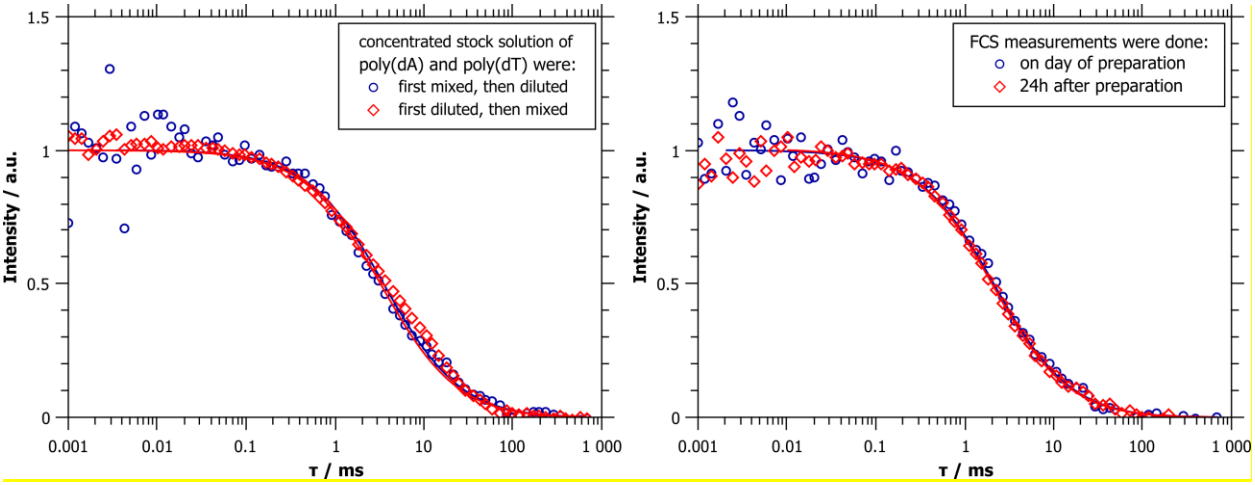

Figure S11. Cross-correlation functions of poly(dAdT) aggregates, showing that different preparation pathways (left) or different incubation time (right) of the sample all lead to the same network structures, hence, the observed sample is in equilibrium.

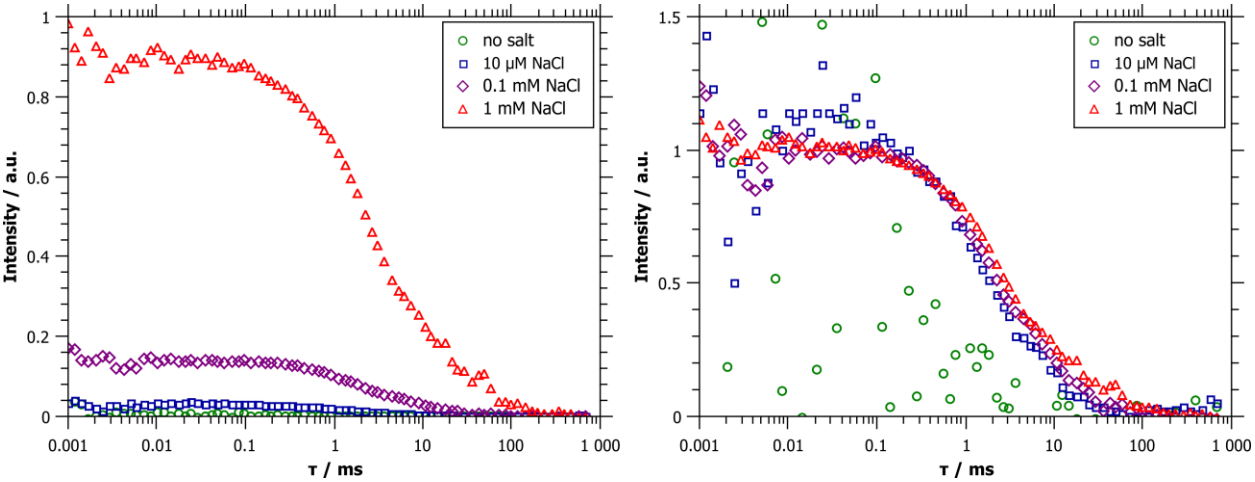

Figure S12. Cross-correlation functions of poly(dAdT) aggregates. The ssDNA solutions were carefully dialyzed after synthesis to remove all remaining salt. Different amounts of NaCl were added to the samples after mixing. Left: original data, right: normalized data for better comparison. The cross-correlation of the 'no salt-sample' is extremely noisy which indicates a weak cross-correlation signal (and thereby the absence of poly(dAdT) aggregates). A sufficiently strong cross-correlation was only found after addition of 10 µM NaCl.